Conference Paper, Published Version

Ata, Riadh

TELEMAC-2D new finite volume schemes for shallow water equations with source terms on 2D unstructured grids

TELEMAC-2D new finite volume schemes for shallow water equations with source terms on 2D unstructured grids

Riadh Ata
EDF-R&D- LNHE
Saint-Venant Laboratory for Hydraulics
6 Quai Watier, Bat. I, Chatou, 78400, France.
riadh.ata@edf.fr

***Abstract*—We present the newly added (in TELEMAC-2D) finite volume schemes (Zokagoa, Tchamen, HLLC and WAF), which give the possibility for users to choose the scheme suited for each kind of application. Depending on the chosen scheme, several interesting numerical properties are obtained. Indeed, the mass conservation, the positivity of water depth, wetting and drying, shock capturing and small numerical diffusion are proved and/or observed. The treatment of a tracer transport in a coupled/split way is not implemented yet and will be the subject of future developments.**

I. INTRODUCTION

We try in this paper to present briefly the new finite volumes (FV) schemes added to TELEMAC-2D in version V6P1 and V6P2. We aim to give a theoretical base for users to understand the algorithmic and the implementation aspects in order to help them toward an optimal use.

We do not claim a complete originality through this work. Indeed, the HLLC, for instance, is a well-known and a widely used scheme. Nevertheless, the remaining schemes are introduced on a vertex-centered 2D unstructured meshes for the first time (as far as we know). Moreover, some major numerical novelties dealing with the WAF scheme are introduced for the first time and are an exclusivity of TELEMAC-2D.

II. TELEMAC-2D FINITE VOLUMES FRAMEWORK

A. The Saint Venant equations

We recall the Saint-Venant equations written in a conservative form:

$$\frac{\partial \boldsymbol{U}}{\partial x}+\frac{\partial \boldsymbol{G}(\boldsymbol{U})}{\partial x}+\frac{\partial \boldsymbol{H}(\boldsymbol{U})}{\partial x}=\boldsymbol{S}(\boldsymbol{U})\ on\ \Omega\times[0,\mathrm{T_s}]$$

where $\boldsymbol{U}=\begin{bmatrix}h\\hu\\hv\end{bmatrix}, \boldsymbol{G}(\boldsymbol{U})=\begin{bmatrix}hu\\hu^2+\frac{1}{2}gh^2\\huv\end{bmatrix}$,

$$\boldsymbol{H}(\boldsymbol{U})=\begin{bmatrix}hu\\huv\\hv^2+\frac{1}{2}gh^2\end{bmatrix}, \boldsymbol{S}(\boldsymbol{U})=\begin{bmatrix}0\\gh(S_{0x}-S_{fx})\\gh(S_{0y}-S_{fy})\end{bmatrix},$$

$$\boldsymbol{S_0}=\begin{bmatrix}\boldsymbol{S_{0x}}=\frac{\partial z}{\partial x}\\\boldsymbol{S_{0y}}=\frac{\partial z}{\partial y}\end{bmatrix}, \boldsymbol{S_f}=\begin{bmatrix}\boldsymbol{S_{fx}}=\frac{n^2u\sqrt{u^2+v^2}}{h^{\frac{4}{3}}}\\\boldsymbol{S_{fy}}=\frac{n^2v\sqrt{u^2+v^2}}{h^{\frac{4}{3}}}\end{bmatrix}$$

where h=η-z is the water depth, η is the free surface, z is the bathymetry, (u,v) are the x and y components of the velocity, g is the gravity acceleration, n is the Manning roughness coefficient and T_s is the simulation time.

This system is widely studied in the literature, we recall here some of its main properties:

- It is strictly hyperbolic for h>0 and loses its hyperbolicity for h=0. This means that water depth could vanish and dry areas may appear in the domain.
- It has an entropy inequality ($\tilde{\alpha}$) related to physical energy (α):

$$\frac{\partial \tilde{\alpha}(U)}{\partial t}+\frac{\partial \tilde{G}(U)}{\partial x}\leq 0$$

where $\alpha(U)=\frac{hu^2}{2}+\frac{gh^2}{2}, G(U)=\left(\frac{hu^2}{2}+gh^2\right)u,$

$\tilde{\alpha}(U,z)=\alpha(U)+hgz, \tilde{G}(U,z)=G(U)+hgzu$

- It admits non trivial steady states, such as the lake at rest (i.e. h+z=cst for u=0).

B. The finite volume framework

We present here the general framework of the finite volume approach used for all the schemes of TELEMAC-2D. The entire domain Ω is subdivided into N sub-domains called control volumes K_i associated to a vertex i. In TELEMAC-2D, we use a vertex-centred approach based on "dual mesh". Specifically, the dual cell is obtained by joining the centres

of mass of the triangles T_i surrounding the vertex i, see Fig. 1.

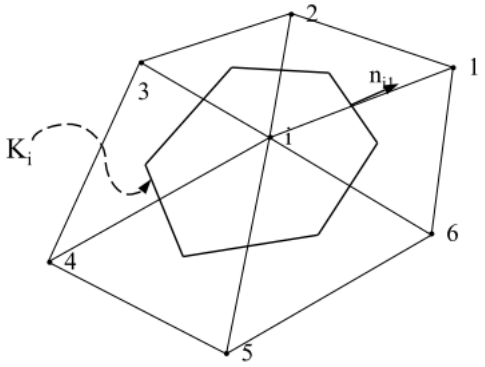

Figure 1. Finite volume framework in TELEMAC-2D

After integration over the control volume defined by Fig. 1 and using the Gauss theorem, last equation gives:

$$U^{n+1} = U^n - \sum_{j=1}^{m_i} \sigma_{ij} F\left(U_i^n, U_j^n, n_{ij}\right) - \sigma_{ij} F(U_i^n, U_e^n, n_i) + \Delta t\, S_i^n$$

where $F\left(U_i^n, U_j^n, n_{ij}\right)$ is an estimation of the normal component of the flux $F(U).n$ along the edge Γ_{ij} separating the nodes i and j.

To have a finite volume method, it is enough to prescribe a numerical flux *F* and a numerical source term S_i.

III. PRESENTATION OF THE NEW SCHEMES

In TELEMAC-2D, there exists already Roe and (first and second order in space) kinetic schemes. We will not present these two schemes in this paper. We will focus only on the newly added schemes, i.e. Zokagoa, Tchamen, HLLC and WAF.

A. Zokagoa and Tchamen schemes

We present these two schemes together since they make similar assumptions and have similar formulations of their numerical fluxes. The peculiarity of these schemes is that the numerical flux is calculated assuming a new set of unknowns where the first component is the free surface elevation η and no more the water depth h. They are recommended for problems with important wetting and drying sequences. See [4] for more details.

These two schemes are based on the discretisation of the geometrical source term $g \int_{K_i} h\nabla z\, d\Omega$. Substituting z by η − h gives:

$$\int_{K_i} h\nabla z\, d\Omega = \int_{K_i} h\nabla\eta\, d\Omega - \int_{K_i} \frac{1}{2} h\nabla \mathrm{h}^2\, d\Omega$$

Since $\int_{K_i} \frac{1}{2} h\nabla \mathrm{h}^2\, d\Omega$ exists in the advection part, the geometrical source term becomes:

$$\mathbf{S}_{\mathrm{b_i}} = \int_{K_i} gh\nabla\eta\, d\Omega$$

Several strategies could be used for the discretisation of this integral. We give hereafter the ideas of Tchamen and Zokagoa:

- Tchamen proposed a local linearisation of Sbi: $S_{b_i} = \bar{h} \int_{K_i} g\nabla\eta\, d\Omega$, where $\bar{h}$ is a mean value of the water depth in the cell, defined with respect to conservation properties and interface states (wet/dry).
- Zokagoa proposed a nonlinear model derived in order to compute more accurately the propagation of discontinuities. The water depth is substituted by the difference between the free surface and the bottom levels: h=η−z, but with the constraint h=η−z> 0, which gives:

$$S_{b_i} = \int_{K_i} gh\nabla\eta\, d\Omega = \int_{K_i} gh\nabla\frac{\eta^2}{2} d\Omega - \int_{K_i} gz\nabla\eta d\Omega .$$

In a similar way, by assuming $z = \bar{z}$ on the control volume, the source term is approximated as: $S_{b_i} \approx g \int_{K_i} \nabla\left(\frac{\eta^2}{2} - \overline{z\eta}\right) d\Omega$

The final fluxes are given by:

$$\mathcal{F}_{\mathbf{ij}}(\mathbf{V_i}, \mathbf{V_j}, \mathbf{n_{ij}}) = \frac{1}{2}\begin{bmatrix} h_i u_{i,n} + h_j u_{j,n} \\ h_i u_{j,n}^2 + g h_i(\eta_i + \eta_j) \\ h_i u_{i,n} v_{i,n} + h_j u_{j,n} v_{j,n} \end{bmatrix}$$

$$- \frac{1}{2} D_{ij} \begin{bmatrix} \eta_j - \eta_i \\ h_j u_{j,n} - h_i u_{i,n} \\ h_j v_{j,n} - h_i v_{i,n}, \end{bmatrix}$$

where $u_{k,n} = u_k n_{ij}^x + v_k n_{ij}^y$ and $v_{k,n} = v_k n_{ij}^x + u_k n_{ij}^y$. In TELEMAC-2D, two choices are possible for the updwinding D_{ij}:

- Toro's choice (default): $D_{ij} = max\{|u_{i,n}| + \sqrt{gh_i}\,, |u_{j,n}| + \sqrt{gh_j}\}$
- Zokagoa's choice: $D_{ij} = \lambda_{ij} = \alpha\, max\{|\tilde{u}_{i,n} - \tilde{c}_{i,n}|, |u_{j,n}|, |\tilde{u}_{i,n} + \tilde{c}_{i,n}|\}$, where $0 \le \alpha \le 1$, $\tilde{u}_{i,n} = \frac{u_{i,n} + u_{j,n}}{2}$ and $\tilde{c}_{i,n} = \sqrt{\frac{h_i + h_j}{2}}$

B. HLLC scheme

The HLLC (C standing for Contact, the missing intermediate wave) is an amelioration proposed by Toro et al.[1] of the basic HLL (Harten, Lax, van Leer) scheme. Indeed, the HLL scheme requires estimates of the wave speeds S_L and S_R of the left and right waves present in the

solution of the Riemann problem defined with data $U_L = U_i^n$, $U_R = U_{i+1}^n$ and corresponding fluxes $F_L = F(U_L)$, $F_R = F(U_R)$ (see Fig. 2). To consider the effect of the intermediate waves, such as shear waves and contact discontinuities, another intermediate speed, called S_*, has to be considered.

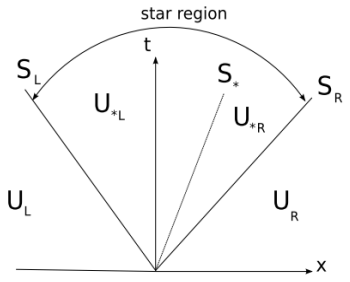

Figure 2. Structure of the solution of the Riemann problem described above.

The general solution of the Riemann problem defined above is:

$$\tilde{\mathbf{U}}(x,t) = \begin{cases} \mathbf{U_L}, & \text{if} \quad \frac{x}{t} \leq S_L \\ \mathbf{U_{*L}}, & \text{if} \quad S_L \leq \frac{x}{t} \leq S_* \\ \mathbf{U_{*R}}, & \text{if} \quad S_* \leq \frac{x}{t} \leq S_R \\ \mathbf{U_R}, & \text{if} \quad \frac{x}{t} \geq S_R \end{cases}$$

The three star states are:

$$\boldsymbol{U}_{*K} = h_K \left(\frac{S_K - U_K}{S_K - S_*} \right) \begin{bmatrix} 1 \\ S_* \\ v_K \end{bmatrix}$$

with k = L,R.

The corresponding HLLC flux is:

$$\mathcal{F}_{i+\frac{1}{2}}^{hllc} = \begin{cases} \mathbf{F_L}, & \text{if} \quad 0 \leq S_L \\ \mathbf{F_{*L}}, & \text{if} \quad S_L \leq 0 \leq S_* \\ \mathbf{F_{*R}}, & \text{if} \quad S_* \leq 0 \leq S_R \\ \mathbf{F_R}, & \text{if} \quad 0 \geq S_R \end{cases}$$

The star components of the flux can be obtained, for instance by applying the Rankine-Hugoniot condition for each of the waves; which gives:

$$\mathbf{F}_{*L} = \mathbf{F}_L + S_L(\mathbf{U_{*L}} - \mathbf{U}_L)$$
$$\mathbf{F}_{*R} = \mathbf{F}_{*L} + S_L(\mathbf{U_{*R}} - \mathbf{U}_{*L})$$
$$\mathbf{F}_{*R} = \mathbf{F}_R + S_R(\mathbf{U_{*R}} - \mathbf{U}_R)$$

where the water depth and normal component of the velocity in the star region are given by:

$$h_{*L} = h_{*R} = h_*$$
$$u_{*L} = u_{*R} = u_*$$

and the tangential velocity component:

$$v_{*L} = v_L$$
$$v_{*R} = v_R$$

where

$$h_* = \frac{(h_L + h_R)}{2} - \frac{1}{4}\frac{(u_R - u_L)(h_L + h_R)}{c_R + c_L}$$
$$u_* = \frac{(u_L + u_R)}{2} - \frac{1}{4}\frac{(h_R - h_L)(c_L + c_R)}{h_R + h_L}$$

The detection of a shock or a rarefaction wave is achieved by a comparison between $h_{L,R}$ and h_*

C. Weighted Averaged Flux (WAF) scheme

The WAF method was first introduced by Toro (1989) in [5]. It is assumed to guarantee second order accuracy in time and space. Second order accuracy in space is obtained with no need for data reconstruction.

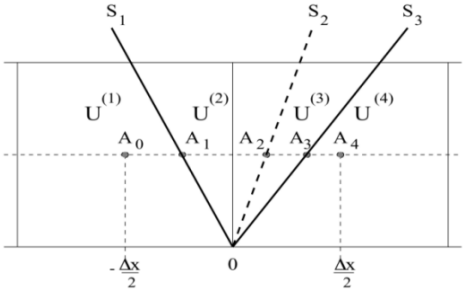

Figure 3. space time (x-t) diagram for the WAF approach.

The original version of the WAF scheme is a weighted sum of the fluxes in all regions of the solution of the piecewise constant data Riemann problem [5], namely:

$$F_{i+\frac{1}{2}} = \frac{1}{\Delta x} \int_{-\frac{\Delta x}{2}}^{\frac{\Delta x}{2}} F\left(U_{i+\frac{1}{2}}\left(x, \frac{\Delta t}{2}\right)\right) dx$$

where $U_{i+\frac{1}{2}}(x,t)$ is the solution of the Riemann problem defined in the previous section. The second order in space and time is obtained since we use one Gauss point to compute this integral (in time and space, i.e. $\frac{\Delta t}{2}$ and $\frac{\Delta x}{2}$).

The integral is therefore easily computed, based on the diagram of Fig. 3, which gives:

$$F_{i+\frac{1}{2}} = \sum_{k=1}^{N+1} \beta_k F_{i+\frac{1}{2}}^{(k)}$$

where $F_{i+\frac{1}{2}}^{(k)} = F\left(U^{(k)}\right)$, $U^{(1)} = U_i^n$, $U^{(2)} = U_L^*$, $U^{(3)} = U_R^*$ and $U^{(4)} = U_{i+1}^n$, N is the number of waves in the solution of the Riemann problem, $\beta_k (k = 0, \ldots, N)$ are the normalised lengths of segments A_kA_{k+1}, which correspond to the difference between the local Courant numbers c_k for successive wave speeds S_k:

$$\beta_k = \frac{|A_k A_{k+1}|}{\Delta x} = \frac{1}{2}(c_k - c_{k-1})$$

$$c_k = \frac{\Delta t S_k}{\Delta x},\ c_0 = -1\ and\ c_{N+1} = 1$$

The generalisation of the WAF description to 2D unstructured meshes in a proper way was achieved by Ata et al.[2]. The procedure cannot be explained in details within this paper, however, it can be summarised as the following: it consists on the writing, in a 2D finite volume framework, the final expression of the discretised SWE combined with a TVD extension to prevent any spurious oscillations in the vicinity of steep gradient.

IV. BOUNDARY CONDITIONS AND TIME DISCRETISATION

We need to define the status U_e, which represents the state in a fictitious cell adjacent to the boundary. In the case of a solid wall, we impose a perfect slipping condition in order to obtain the continuity of the tangential component. In the case of a liquid boundary, we need to distinguish two sub-cases: the subcritical and super-critical cases. It is necessary to specify for every point along the boundary, a number of conditions which depends on the regime: For a subcritical input or output, only one boundary condition (h or Q) is necessary, since there is one characteristic starting within the domain and directed to the entry. For a super-critical input, two conditions (h and Q) are required, while for a supercritical outlet, there is no need for any condition.

For time discretisation, a Newmark scheme is implemented which offers the possibility to retrieve, depending on user choice, a first or a second order accurate scheme.

V. SOURCE TERM TREATMENT

The geometric source term is discretised, as for kinetic schemes, using the hydrostatic reconstruction of Audusse et al. This fundamental aspect ensures the positivity of water depth, the conservation of mass, the well-balanceness (or C-property). More details can be found in [2].

For the discretisation of the friction term, a semi-implicit algorithm is implemented. The friction term is written as:

$$S_f \approx \frac{|q_i^n| q_i^{n+1}}{K^2 h_i^n (h_i^{n+1})^{\frac{4}{3}}}$$

This discretisation is very robust and handles well probable instabilities caused by possible abrupt changes in water depths and velocities.

VI. ASSESSMENT AND VALIDATION

Even though we have achieved a large set of validation cases, we will present here only three of them showing the major good numerical properties of these schemes.

A. C-property

The well-balanceness or C-property is an essential criterion that every numerical scheme should satisfy. In our case, we chose the benchmark proposed by Goutal et al.[2]. It represents a 2D channel with a severe variation of the bathymetry in the longitudinal direction. The schemes have to maintain a lake at rest for a long simulation time. In our case, we fixed a t_{max}= 1000s. The results (water elevation and velocity) are presented in Fig. 4.

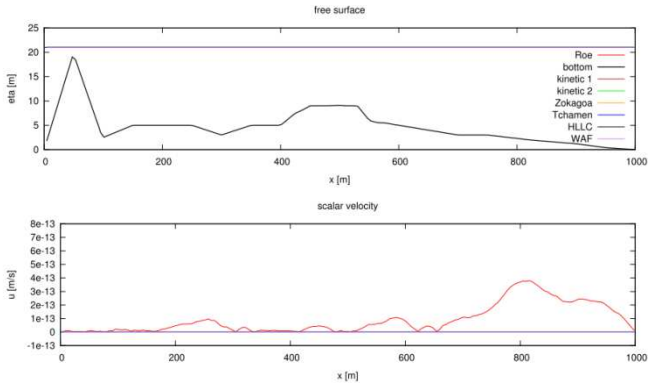

Figure 4. Lake at rest test case - comparison between all the schemes of TELEMAC-2D.

We can conclude, from Fig. 4, that the C-property is well satisfied for all the schemes.

B. Wet and dry dambreak

The second test case is the theoretical dam break with wet (Stoker problem) and dry (Ritter) downstream. These tests permit to ass the shock-capturing capabilities of the schemes and to quantify the numerical diffusion which is located mostly in the shock areas. Initial conditions are defined by water depths of 4m and 1m (or 0m for Ritter case) respectively upstream and downstream of the dam. This latter is located at x=1000m. Figs. 5 and 6 show the obtained results which prove that WAF scheme gives excellent results comparing to the analytical solution and to other schemes.

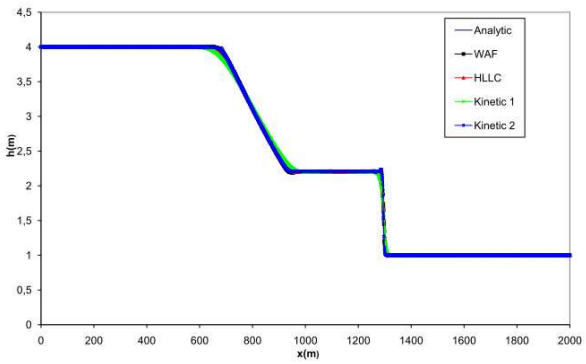

Figure 5. Stoker problem: comparison of water depth and obtained by each scheme.

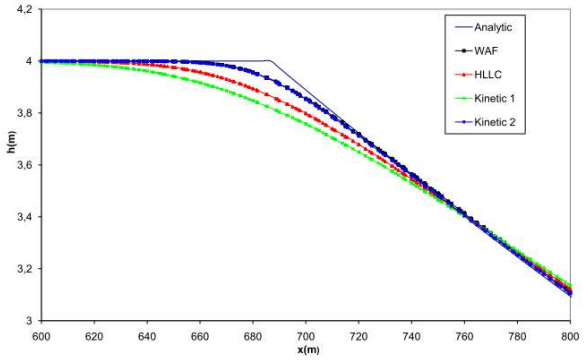

Figure 6. Stoker problem: comparison of water depth zoom on the rarefaction wave that shows the numerical diffusion of each scheme.

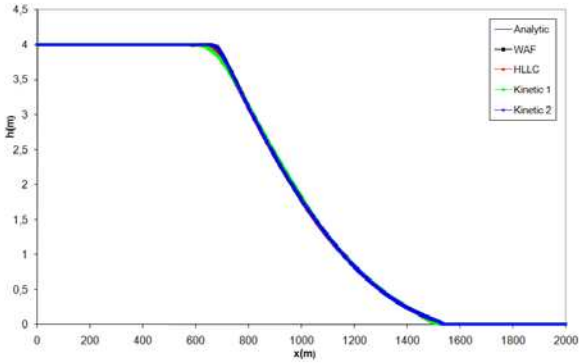

Figure 7. Ritter problem: Comparison between all the FV schemes.

C. *Malpasset dam break*

The last validation case is the real case of Malpasset dam break. All the details about this problem as well as the reference solution are given in [2]. This problem is interesting since it allows to see how the schemes behaves in case of real case which include almost all the numerical challenges (shock-capturing, wetting and drying, steep bathymetry etc.).

The used mesh contains 5435 nodes and 10049 elements. The CFL number is fixed to 0.8 and the Strickler number is assumed to be 30 everywhere in the domain. The simulation time is 4000s. The water depth at several times is shown in Figs. 8, 9 and 10.

The CPU time for some of the schemes is given in the following table (we used a 8-Core HP Z600, Linux, with 4Go of RAM):

TABLE I. CPU TIME RELATIVE TO THE MALPASSET PROBLEM

	HLLC	Kinetic 1st order	Kinetic 2nd order	WAF
CPU time	46 s	55s	1mn56s	1mn08s

The results were compared with those obtained by real measurements and by a physical reduced order model. A L1-type error was used to quantify the error between obtained results (elevation and arrival times) and reference ones. The results are encouraging especially if we consider the fact that we used a single value of the Strickler coefficient and that we have not proceeded by any calibration step before simulating the case.

VII. CONCLUSIONS AND FUTURE WORKS

We presented in this paper a comparative study of the newly added finite volume schemes of TELEMAC-2D. We showed the specific aspects of each scheme and its recommended application. Moreover, we presented a numerical assessment of these schemes through some theoretical and real test cases. The obtained results are very encouraging since we obtained very interesting numerical properties such as positivity of water depth, mass conservation, very nice shock-capturing, low numerical diffusion and very robust wetting and drying treatment. These encouraging results open wide perspectives to apply such formulation in specific applications that need strong and robust numerical properties such as the transport of passive tracer and sediments.

ACKNOWLEDGEMENT

A part of the validation cases showed in this paper were achieved during the training of S. Pavan. The author would like to acknowledge her contribution to this work.

REFERENCES

[1] E.F. Toro, M. Spuce and W. Speares, “Restoration of the contact surface to the Harten-Lax-van der Leer solver”. Journal of Shock Waves,(4) 25-34, 1994.

[2] R. Ata, S. Pavan, S. Khelladi and E.F. Toro, “WAF approximation for shallow water equations with friction and real topography”. Submitted.

[3] S.J. Billett and E.F. Toro, “WAF-Type Schemes for Multidimensional Hyperbolic Conservation Laws” .J. Comput. Physics, Vol.130, pp.1-24.

[4] J.M. Zokagoa., A. Soulaimani. “Modeling of wetting-drying transition in free surface flows over complex topographies.” Computer Methods in Applied Mechanics and Engineering, Vol.199, pp.2281-2304, 2010.

[5] E.F. Toro. A Weighted Average Flux Method for Hyperbolic Conservation Laws (1989). Proc. Roy.Soc.London, (423) 401-418

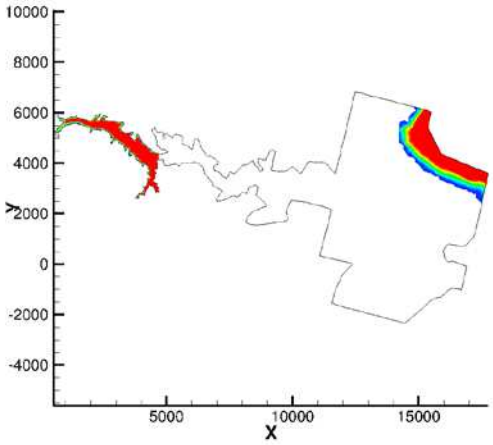

Figure 8. Malpasset dam break initial conditions t=0s.

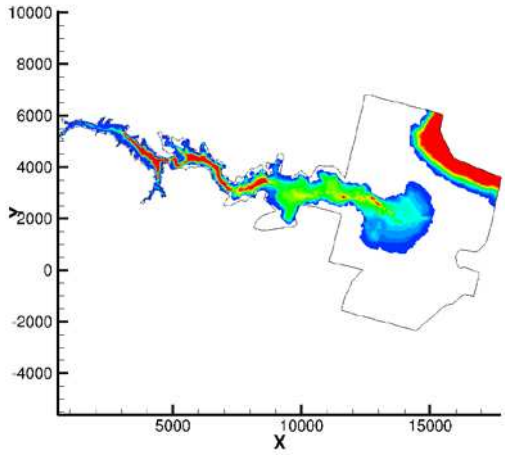

Figure 9. Malpasset dam break: elevation at t=2450s.

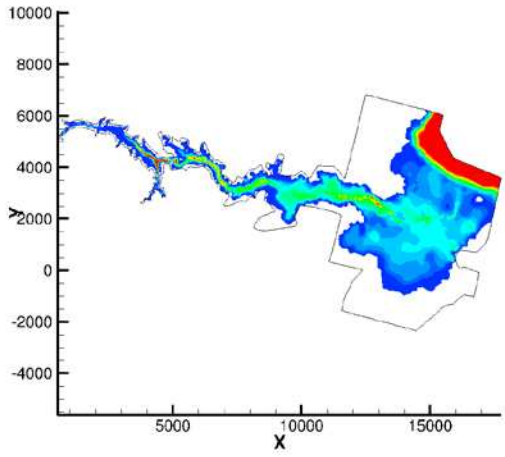

Figure 10. Malpasset dam break: elevation at t=4000s